Pre-Steady-State Kinetic Studies of Protein-Template-Directed Nucleotide Incorporation by the Yeast Rev1 Protein†

Craig A. Howell,‡ Satya Prakash,§ and M. Todd Washington*,‡

Department of Biochemistry, University of Iowa College of Medicine, Iowa City, Iowa 52242-1109, and Department of Biochemistry and Molecular Biology, University of Texas Medical Branch at Galveston, Galveston, Texas 7755-1061

Received July 20, 2007; Revised Manuscript Received September 6, 2007

ABSTRACT: The yeast Rev1 protein (Rev1p) is a member of the Y family of DNA polymerases that specifically catalyzes the incorporation of C opposite template G and several types of DNA damage. The X-ray crystal structure of the Rev1p−DNA−dCTP ternary complex showed that Rev1p utilizes an unusual mechanism of nucleotide incorporation whereby the template residue is displaced from the DNA double helix and the side chain of Arg-324 forms hydrogen bonds with the incoming dCTP. To better understand the impact of this protein-template-directed mechanism on the thermodynamics and kinetics of nucleotide incorporation, we have carried out pre-steady-state kinetic studies with Rev1p. Interestingly, we found that Rev1p's specificity for incorporating C is achieved solely at the initial nucleotide-binding step, not at the subsequent nucleotide-incorporation step. In this respect, Rev1p differs from all previously investigated DNA polymerases. We also found that the base occupying the template position in the DNA impacts nucleotide incorporation more at the nucleotide-binding step than at the nucleotide-incorporation step. These studies provide the first detailed, quantitative information regarding the mechanistic impact of protein-template-directed nucleotide incorporation by Rev1p. Moreover, on the basis of these findings and on structures of the unrelated *Escherichia coli* MutM DNA glycosylase, we suggest the possible structures for the ternary complexes of Rev1p with the other incoming dNTPs.

Classical DNA polymerases synthesize DNA with high efficiency and fidelity. They do this by monitoring the geometric shape of the base pair formed when the incoming nucleotide pairs with the template residue (*1*). This ensures that only the incoming nucleotide forming the correct Watson−Crick base pair with the template base is incorporated. This basis of incoming nucleotide selection precludes these polymerases from efficiently incorporating nucleotides opposite most DNA lesions, because of the geometric distortions they confer. Consequently, classical polymerases usually stall upon encountering a DNA lesion in the template strand. To overcome replication blocks caused by such lesions, cells possess a number of specialized DNA polymerases capable of efficiently incorporating nucleotides opposite DNA damage (*2*−*4*). Many of these specialized enzymes are members of the Y family of DNA polymerases (*3*, *4*), and they utilize a variety of mechanisms for incorporating nucleotides opposite DNA lesions.

DNA polymerases η (pol η) and κ (pol κ) are Y family polymerases, and like classical polymerases, both utilize Watson−Crick base-pairing between the incoming nucleotide and the template residue as the basis for incoming nucleotide selection (*5*−*7*). Even though pol η does not monitor the geometry of the nascent base pair as strictly as classical polymerases do (*8*−*10*), it is still able to utilize the intrinsic Watson−Crick base-pairing abilities of *cis*−*syn*-thymine dimer (*9*−*11*) and 8-oxoguanine lesions (*12*, *13*) to efficiently and accurately incorporate nucleotides opposite these lesions. The X-ray crystal structure of yeast pol η has suggested that this tolerance of deviant DNA geometries is likely due to a more spacious active site compared to those of classical polymerases (*14*). Pol κ, by contrast, does not readily incorporate nucleotides opposite DNA lesions, but it participates in the replication of damaged DNA by extending from nucleotides incorporated opposite DNA lesions by other DNA polymerases (*15*−*17*). The X-ray crystal structure of the ternary complex of human pol κ bound to DNA and an incoming nucleotide shows that this enzyme also utilizes Watson−Crick base-pairing as the basis for incoming nucleotide selection (*7*, *18*).

DNA polymerase ι (pol ι), another Y family polymerase, is able to promote synthesis past several DNA lesions, including abasic sites (*19*, *20*), (6−4) photoproducts (*19*−*21*), and minor groove adducts of G residues (*15*, *16*). Several high-resolution X-ray crystal structures of ternary complexes of human pol ι bound to DNA and incoming nucleotides have shown that this enzyme utilizes Hoogsteen base-pairing as the basis for incoming nucleotide selection (*22*, *23*). This conclusion has been further supported by steady-state kinetic studies of pol ι with substrates containing DNA base analogs that specifically disrupt either Watson−Crick base-pairing or Hoogsteen base-pairing (*24*, *25*). Hoogsteen base-pairing in the active site of pol ι could allow it to incorporate

† This research was supported by Research Scholar Grant #RSG-05-139-01-GMC from the American Cancer Society (to M.T.W.) and by National Institutes of Health Grant CA115856 (to S.P.).

* To whom correspondence should be addressed. Phone: 319-335-7518. Fax: 319-335-9570. E-mail: todd-washington@uiowa.edu.

‡ University of Iowa College of Medicine.

§ University of Texas Medical Branch at Galveston.

10.1021/bi701429v CCC: $37.00
Published on Web 10/26/2007

nucleotides opposite DNA lesions that are unable to form Watson−Crick base pairs (*26*) or that cause serious perturbations in the DNA minor groove (*15*, *16*).

The Rev1 protein (Rev1p[1]), also a member of the Y family of polymerases, could promote synthesis opposite DNA lesions such as an abasic site (*27*−*31*) and minor-groove adducts of G residues (*30*, *32*). Rev1p is unique because it utilizes a protein-template-directed mechanism of incoming nucleotide selection (*33*). The X-ray crystal structure of the ternary complex of yeast Rev1p bound to DNA and dCTP shows that the base occupying the template position is displaced from the DNA double helix, and the side chain of Arg-324 forms hydrogen bonds with the incoming dCTP (*33*). This mechanism allows Rev1p to select the incoming nucleotide without this nucleotide contacting the DNA template.

Previous steady-state kinetic studies showed that Rev1p preferentially incorporates C opposite template G and the various DNA lesions (*28*−*32*). Moreover, opposite templates A, T, and C, the preferred incoming nucleotide remains dCTP (*29*−*31*). While steady-state kinetic studies are appropriate for quantifying the preference of Rev1p for one incoming nucleotide over another, these studies do not address the mechanism of incoming nucleotide selection. For example, these studies do not show at which step, the initial nucleotide-binding step or the subsequent nucleotide-incorporation step, Rev1p selects for the incoming nucleotide. This is a particularly important question given the unique protein-template-directed mechanism employed by this enzyme.

To better understand the mechanism of nucleotide selection by Rev1p, we have carried out pre-steady-state kinetic studies with this enzyme. We show that unlike all other polymerases examined to date, incoming nucleotide selection is accomplished solely at the initial nucleotide-binding step and not at the subsequent nucleotide-incorporation step. Thus, specificity for nucleotide incorporation is achieved by the differential ground state binding affinities of various dNTPs for the Arg-324 side chain. Also, we found that the identity of the extrahelical base in the DNA substrate occupying the template position impacts nucleotide incorporation more at the nucleotide-binding step than at the nucleotide-incorporation step. These studies provide the first detailed, quantitative information regarding the mechanistic impact of protein-template-directed nucleotide incorporation by Rev1p.

EXPERIMENTAL PROCEDURES

Purification of Rev1p. Yeast Rev1p was expressed in yeast strain BJ5464 carrying plasmid pRev1.41, which encodes Rev1p (amino acids 1−746) fused in frame with glutathione-*S*-transferase (GST) gene. The N-terminal GST-Rev1p fusion protein was purified, and the GST portion was removed by treatment with PreScission protease (GE Healthcare) as previously described (*34*). The full length Rev1p comprises 985 amino acid residues, so the resulting protein is missing 239 amino acid residues from its C-terminus. However, this truncated protein is as active in DNA synthesis as the full length wild-type protein (data not shown). We will refer to this truncated protein as Rev1p throughout this paper. Purified Rev1p protein was stored at −80 °C in 10 μL aliquots. The concentration of purified protein was determined using the Bio-Rad assay with BSA as the standard.

DNA and Nucleotide Substrates. The DNA substrates were comprised of two synthetic oligodeoxynucleotides annealed together. The same 24-mer primer sequence, 5′-GCC TCG CAG CCG TCC AAC CAA CTC, was used for all experiments. Six 45-mer templates were used with the sequence 5′-GGA CGG CAT TGG ATC GAC CTX GAG TTG GTT GGA CGG CTG CGA GGC. The X is a G, A, T, C, abasic site, or 8-oxoguanine. The oligonucleotides containing the abasic site and the 8-oxoguanine were synthesized by Midland Certified Reagent Co., Inc. The other oligonucleotides were synthesized by Integrated DNA Technologies, Inc. The primer strand was 5′-^{32}P end-labeled with T4 polynucleotide kinase (New England Biolabs) and [γ-^{32}P]-ATP (6,000 Ci/mmol; Perkin-Elmer) at 37 °C for 1 h. Labeled primer strands were separated from unused [γ-^{32}P]-ATP with a Sephadex G-25 spin column (Amersham BioSciences). The labeled primer strands were annealed to template strands in 50 mM Tris Cl and 100 mM NaCl by heating at 90 °C for 2 min and slow cooling to room temperature over several hours. Annealed strands were stored at 4 °C for up to 2 weeks. Solutions of each dNTP (100 mM, sodium salt) were obtained from New England Biolabs and stored in aliquots at −80 °C.

Single Turnover Experiments. All polymerase reactions were measured in 25 mM TrisCl (pH 7.5), 5 mM $MgCl_2$, 5 mM dithiothreitol, and 10% glycerol at 22 °C. Rev1p (100 nM final concentration) was preincubated for several minutes at 22 °C with the labeled DNA substrate (100 nM final concentration) and then mixed with a single dNTP (0−1000 μM final concentration) to initiate the reaction. Samples were quenched after various reaction times with formamide loading buffer (80% deionized formamide, 10 mM EDTA, 1 mg/mL xylene cyanol, and 1 mg/mL bromophenol blue). Extended primer strands (the products) were separated from unextended primer strands (the substrates) on a 15% polyacrylamide sequencing gel containing 8 M urea. The labeled gel bands were quantified with the InstantImager (Packard). Each set of DNA and dNTP concentrations was repeated several times to ensure reproducibility.

Data Analysis. To determine the observed first-order rate constant for nucleotide incorporation (k_{obs}), the concentrations of product formed (P) were graphed as a function of time (t), and the data were fit by nonlinear regression (SigmaPlot 8.0) to the exponential equation

$$P = A(1 - \exp(-k_{obs}t))$$

where A (the amplitude of the exponential phase) was fixed at 100 nM.

To determine the dissociation constant (K_d) for the nucleotide-binding step and the maximum first-order rate constant for nucleotide incorporation (k_{pol}), the observed rate constants (k_{obs}) were graphed as a function of dNTP concentration ([dNTP]), and the data were fit by nonlinear regression to the hyperbolic equation

$$k_{obs} = k_{pol}[\text{dNTP}]/(K_D + [\text{dNTP}])$$

[1] Abbreviations: Rev1p, the Rev1 protein; pol, polymerase; GST, glutathione-*S*-transferase; dNTP, deoxynucleoside triphosphate; 8-oxoG, 8-oxoguanine; EDTA, ethylenediaminetetraacetic acid.

RESULTS

Rev1p utilizes a unique protein-template-directed mechanism of nucleotide incorporation in which the side chain of Arg-324 forms hydrogen bonds with the incoming dCTP. To better understand the impact of this protein-template-directed mechanism on the thermodynamics and kinetics of nucleotide incorporation, we have carried out pre-steady-state kinetic studies with Rev1p. To understand the basis of incoming nucleotide selection, we have examined the kinetics of incorporation of all four dNTPs in the presence of a DNA substrate with a G at the template position. Furthermore, to understand the impact of the type of base at the template position in the DNA, we have examined the kinetics of C incorporation opposite all four undamaged bases and opposite an abasic site and an 8-oxoguanine lesion.

Kinetics of C Incorporation Opposite G. Using single turnover experiments, we examined the mechanism of C incorporation with a DNA substrate containing a G in the template position, which is the optimal substrate for this enzyme. By contrast to steady-state kinetics, where the substrate concentrations are in vast excess over the enzyme concentration, single turnover experiments utilize concentrations of enzyme greater than or equal to substrate concentration. Consequently, all substrate is converted to product in a single enzyme turnover. In these experiments, we preincubated 100 nM ^{32}P-end labeled DNA and 100 nM Rev1p, initiated the reaction by adding 5 μM dCTP, and then quenched aliquots after various reaction times ranging from 20 to 300 s. The amounts of product formed were plotted as a function of time (Figure 1A), and the data were fit to an equation describing a single exponential (see Experimental Procedures) with an observed first-order rate constant (k_{obs}) equal to 0.014 ± 0.001 s^{-1}.

We carried out an important control experiment in which we added 100 nM of cold, unlabeled DNA to the preincubated ^{32}P-labeled DNA-Rev1p solution at precisely the same time as we initiated the reaction with the dCTP. This control was necessary to ensure that all of the Rev1p was bound to labeled DNA during the preincubation period. The kinetics of product formation in this control experiment was identical to those of the experiments in which the unlabeled DNA was not added (data not shown). This control demonstrated that all Rev1p molecules were indeed bound to labeled DNA prior to addition of dCTP and that the observed rate constant we measured reflects the chemical step of phosphodiester bond formation or a conformational change step in the Rev1p−DNA−dCTP ternary complex that immediately precedes and limits the chemical step.

We next examined the dCTP-concentration dependence of the observed first-order rate constant of nucleotide incorporation. We carried out experiments as described above except that the dCTP concentration was varied from 0.1 to 5 μM (Figure 1B). The observed first-order rate constants (k_{obs}) were plotted as a function of dCTP concentration (Figure 1C), and the data was fit to an equation describing a rectangular hyperbola (see Experimental Procedures). The best fit of these data provided a K_d for the initial dCTP-binding step equal to 0.83 ± 0.07 μM and a maximal first-order rate constant for the subsequent nucleotide-incorporation step (k_{pol}) equal to 0.017 ± 0.005 s^{-1}. Table 1 provides the mean and standard errors of the K_d and k_{pol} values that were determined in multiple independent experiments. The K_d for dCTP binding is typical of what has been observed previously for correct dNTP binding for most other DNA

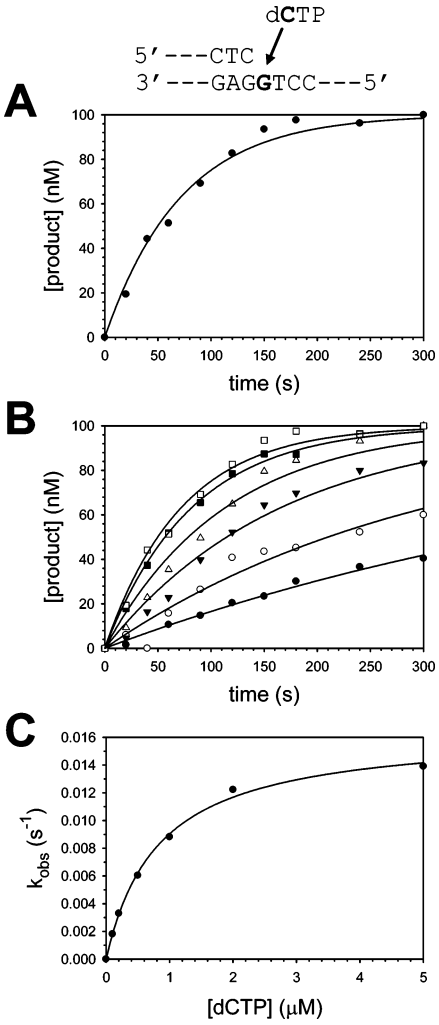

FIGURE 1: Kinetics of C incorporation opposite template G. (A) Preincubated Rev1p (100 nM) and DNA containing a G template (100 nM) were mixed with dCTP (5 μM) for various lengths of time. The data were fit to an exponential equation with k_{obs} equal to 0.014 ± 0.001 s^{-1}. (B) Preincubated Rev1p (100 nM) and DNA containing a G template (100 nM) were mixed with dCTP (0.1 μM, closed circles; 0.2 μM, open circles; 0.5 μM, closed triangles; 1 μM, open triangles; 2 μM, closed squares; 5 μM, open squares) for various lengths of time. The solid lines represent the best fits to the exponential equation. (C) The k_{obs} values were graphed as a function of dCTP concentration, and the solid line represents the best fit to the hyperbolic equation with k_{pol} equal to 0.017 ± 0.005 s^{-1} and K_d equal to 0.83 ± 0.07 μM.

Table 1: Pre-Steady-State Kinetic Parameters for Nucleotide Incorporation Opposite Template G

dNTP	template	k_{pol}[a] (s^{-1})	K_d[a] (μM)	k_{pol}/K_d (μM^{-1} s^{-1})	f_{rel}[b]
dCTP	G	0.012 ± 0.004	0.78 ± 0.05	0.015	1.0
dGTP	G	0.017 ± 0.003	270 ± 60	6.3×10^{-5}	240
dATP	G	ND[c]	ND	$<1 \times 10^{-6}$	>15000
dTTP	G	0.0036 ± 0.0007	200 ± 70	1.8×10^{-5}	830

[a] Values reported here represent the mean and standard error derived from multiple, independent experiments. [b] f_{rel} is the ratio of k_{pol}/K_d for dCTP incorporation to k_{pol}/K_d for the incorporation of the given nucleotide. [c] Not detectible. In this case, limits for the k_{pol}/K_d and f_{rel} were determined from the estimated detection limit of our assay.

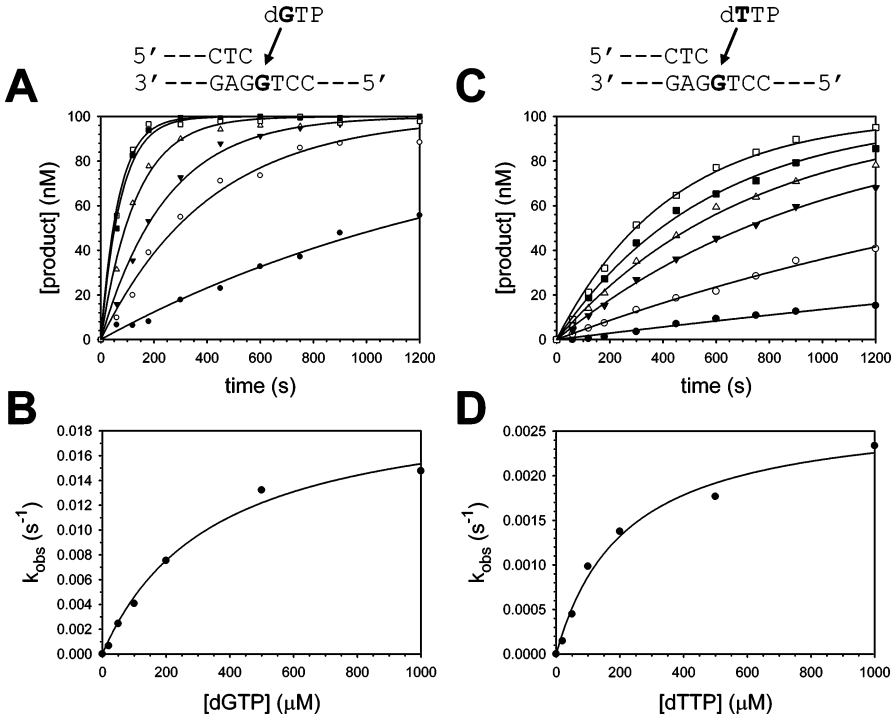

FIGURE 2: Kinetics of other nucleotide incorporation opposite template G. (A) Preincubated Rev1p (100 nM) and DNA containing a G template (100 nM) were mixed with dGTP (20 μM, closed circles; 50 μM, open circles; 100 μM, closed triangles; 200 μM, open triangles; 500 μM, closed squares; 1000 μM, open squares) for various lengths of time. The solid lines represent the best fits to the exponential equation. (B) The k_{obs} values were graphed as a function of dGTP concentration, and the solid line represents the best fit to the hyperbolic equation with k_{pol} equal to 0.021 $\pm$ 0.002 s^{-1} and K_d equal to 350 $\pm$ 60 μM. (C) Preincubated Rev1p (100 nM) and DNA containing a G template (100 nM) were mixed with dTTP (20 μM, closed circles; 50 μM, open circles; 100 μM, closed triangles; 200 μM, open triangles; 500 μM, closed squares; 1000 μM, open squares) for various lengths of time. The solid lines represent the best fits to the exponential equation. (D) The k_{obs} values were graphed as a function of dTTP concentration, and the solid line represents the best fit to the hyperbolic equation with k_{pol} equal to 0.0027 $\pm$ 0.0002 s^{-1} and K_d equal to 220 $\pm$ 40 μM.

polymerases; however, the k_{pol} value for Rev1p is considerably slower than that of other DNA polymerases.

Kinetics of Other Nucleotide Incorporation Opposite G. To better understand the mechanism of incoming nucleotide selection, we next examined the kinetics of incorporation of the other three nucleotides in the presence of a DNA substrate with a G residue at the template position. These experiments were carried out as described above, except that the dGTP and dTTP concentrations were varied from 20 to 1000 μM (Figure 2A,C). The k_{obs} values were determined and were plotted as a function of nucleotide concentration (Figure 2B,D). The K_d and k_{pol} values were determined from the best fits of these data to the hyperbolic equation (see Experimental Procedures). Mean and standard error values from multiple, independent experiments are given in Table 1. These results show that the affinity of dGTP and dTTP for the Rev1p-DNA binary complex is reduced by ~350- and ~260-fold, respectively than for dCTP. Interestingly, the k_{pol} values for G, T, and C incorporation are approximately the same.

We also examined the incorporation of A in the presence of a DNA substrate with a G in the template position. However, we saw no detectable A incorporation under the conditions (up to 2 mM dATP) and time scale (up to 60 min) used in these experiments. On the basis of the estimated detection limit of our assays, we conclude that the efficiency of A incorporation is at least 15 000 lower than that of C incorporation.

Kinetics of C Incorporation Opposite A, T, and C. To better understand the impact of the type of base at the template position in the DNA, we examined the kinetics of C incorporation with an A (Figure 3A,B), a T (Figure 3C,D), or a C at this position (Figure 3E,F). Mean and standard error values for the K_d and k_{pol} determined from multiple, independent experiments are given in Table 2. These results show that the presence of a nonoptimal base in the template position results in either weaker incoming dNTP binding or both weaker incoming dNTP binding and slower incorporation of the nucleotide once it is bound. Thus, for template A, the affinity for binding dCTP was reduced by 130-fold, but the k_{pol} was only ~3-fold slower. For templates T and C, the affinity for binding dCTP was reduced by ~95- and ~45-fold, respectively, and the k_{pol} was slower by ~17- and ~25-fold, respectively.

Kinetics of Incorporation Opposite DNA Lesions. Next, we examined the kinetics of C incorporation opposite an abasic site (Figure 4A,B) and opposite an 8-oxoguanine lesion (Figure 4C,D), and the mean and standard error values for the K_d and k_{pol} are given in Table 2. These results show that the presence of these DNA lesions in the template position results in weaker incoming dNTP binding but has little impact of the rate of the nucleotide-incorporation step. Furthermore, binding of the incoming dCTP is significantly weaker with 8-oxoguanine than with the abasic site.

DISCUSSION

Recent structural and pre-steady-state kinetic studies have shown that members of the Y family of specialized DNA polymerases utilize different mechanisms for selecting an incoming nucleotide to incorporate opposite damaged DNA

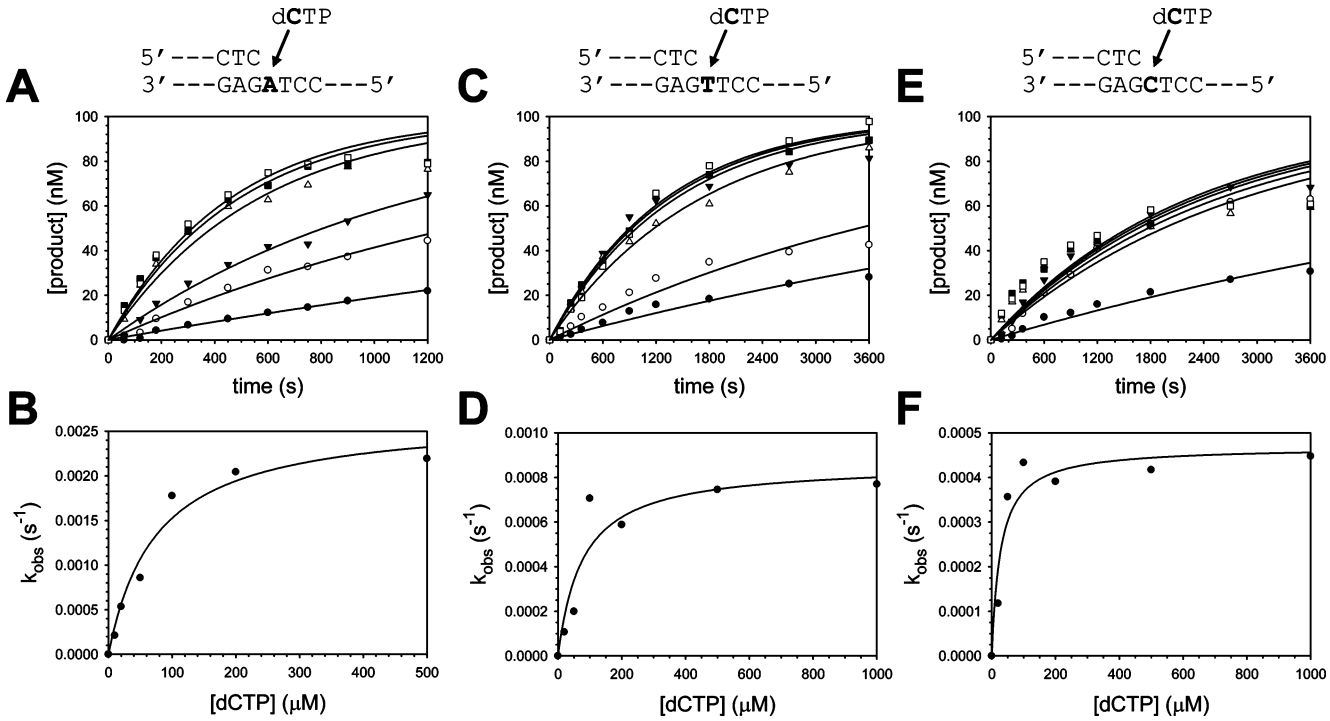

FIGURE 3: Kinetics of C incorporation opposite other templates. (A) Preincubated Rev1p (100 nM) and DNA containing an A template (100 nM) were mixed with dCTP (10 μM, closed circles; 20 μM, open circles; 50 μM, closed triangles; 100 μM, open triangles; 200 μM, closed squares; 500 μM, open squares) for various lengths of time. The solid lines represent the best fits to the exponential equation. (B) The k_{obs} values were graphed as a function of dCTP concentration, and the solid line represents the best fit to the hyperbolic equation with k_{pol} equal to 0.0027 ± 0.0002 s^{-1} and K_d equal to 75 ± 20 μM. (C) Preincubated Rev1p (100 nM) and DNA containing a T template (100 nM) were mixed with dCTP (20 μM, closed circles; 50 μM, open circles; 100 μM, closed triangles; 200 μM, open triangles; 500 μM, closed squares; 1000 μM, open squares) for various lengths of time. The solid lines represent the best fits to the exponential equation. (D) The k_{obs} values were graphed as a function of dCTP concentration, and the solid line represents the best fit to the hyperbolic equation with k_{pol} equal to 0.00090 ± 0.00010 s^{-1} and K_d equal to 77 ± 39 μM. (E) Preincubated Rev1p (100 nM) and DNA containing a C template (100 nM) were mixed with dCTP (20 μM, closed circles; 50 μM, open circles; 100 μM, closed triangles; 200 μM, open triangles; 500 μM, closed squares; 1000 μM, open squares) for various lengths of time. The solid lines represent the best fits to the exponential equation. (F) The k_{obs} values were graphed as a function of dCTP concentration and the solid line represents the best fit to the hyperbolic equation with k_{pol} equal to 0.00046 ± 0.00004 s^{-1} and K_d equal to 27 ± 11 μM.

Table 2: Pre-Steady-State Kinetic Parameters for C Incorporation Opposite Various Templates

dNTP	template	k_{pol}[a] (s^{-1})	K_d[a] (μM)	k_{pol}/K_d (μM^{-1} s^{-1})	f_{rel}[b]
dCTP	G	0.012 ± 0.004	0.78 ± 0.05	0.015	1.0
dCTP	A	0.0036 ± 0.0009	100 ± 30	3.6×10^{-5}	420
dCTP	T	0.00070 ± 0.00020	74 ± 4	9.5×10^{-6}	1600
dCTP	C	0.00048 ± 0.00002	35 ± 7	1.3×10^{-5}	1200
dCTP	Abasic	0.0058 ± 0.0023	36 ± 14	1.6×10^{-4}	94
dCTP	8-oxoG	0.0033 ± 0.0008	220 ± 70	1.5×10^{-5}	1000

[a] Values reported here represent the mean and standard error derived from multiple, independent experiments. [b] f_{rel} is the ratio of k_{pol}/K_d for incorporation opposite template G to k_{pol}/K_d for incorporation opposite the given template.

templates. For example, the X-ray crystal structure of yeast pol η has suggested that it possesses an active site large enough to accommodate DNA lesions such as a *cis*−*syn*-thymine dimer or an 8-oxoguanine (*14*), and this enzyme preferentially incorporates incoming nucleotides that form Watson−Crick base pairs with these lesions. Pre-steady-state kinetic analyses have shown that pol η achieves nucleotide selection at both the nucleotide-binding and nucleotide-incorporation steps (*11*, *13*, *34*). Structural studies have also shown that human pol ι, unlike pol η and all other DNA polymerases examined to date, does not utilize Watson−Crick base-pairing to select the incoming nucleotide. Instead, pol ι rotates the purine template base around the glycosidic bond into the syn conformation and utilizes Hoogsteen base-pairing to direct nucleotide incorporation (*22*, *23*). Despite this highly unusual base-pairing mechanism, pre-steady-state kinetic studies have shown that pol ι, like other DNA polymerases, achieves nucleotide selection at both the nucleotide-binding and nucleotide-incorporation steps (*35*).

The X-ray crystal structure of Rev1p in a ternary complex with DNA and an incoming dCTP has revealed an even more unusual mechanism of selecting the incoming nucleotide (*33*). In Rev1p, the template residue is displaced from the DNA double helix and is replaced by the side chain of Arg-324. The ϵ and ζ nitrogen atoms of the Arg-324 side chain act as hydrogen-bond donors and interact with the and O^2 and N3 hydrogen-bond acceptors on the cytosine base of the incoming dCTP (Figure 5). Thus, Rev1p utilizes a protein-template-directed mechanism to selectively incorporate C opposite G and certain DNA lesions. In this paper, we have carried out pre-steady-state kinetic analyses to determine precisely how and at which steps along the reaction pathway this protein-template-directed mechanism leads to a preference for incorporating C.

While dCTP is always the preferred incoming nucleotide due to hydrogen bonding with Arg-324, previous steady-state kinetic studies showed that the nucleotide in the template position has a marked impact on the efficiency of C incorporation (*29*−*31*). For example, steady-state kinetic

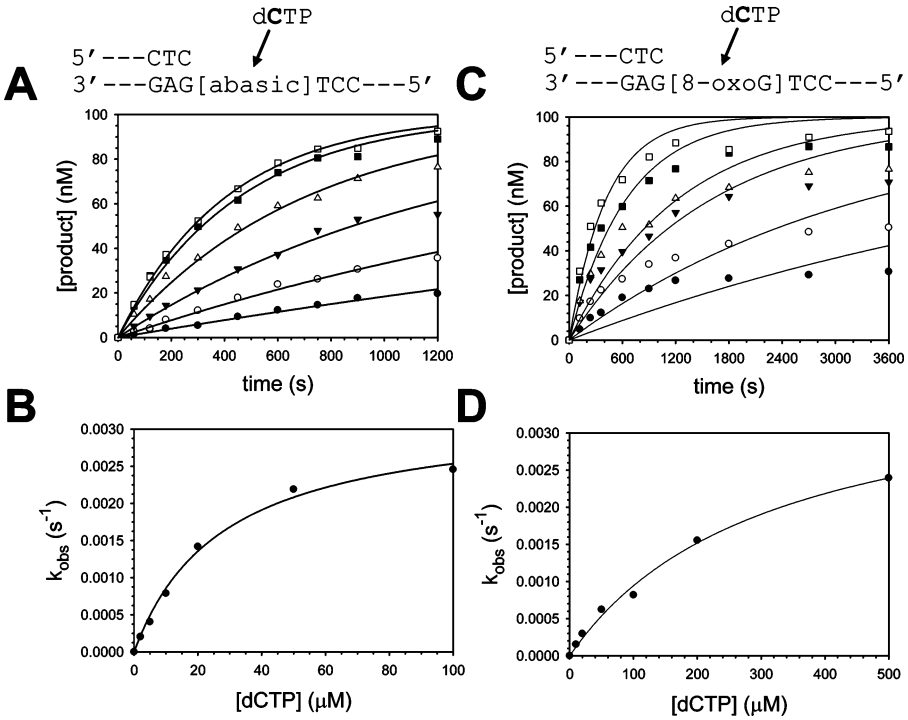

FIGURE 4: Kinetics of C incorporation opposite DNA lesions. (A) Preincubated Rev1p (100 nM) and DNA containing an abasic site template (100 nM) were mixed with dCTP (2 μM, closed circles; 5 μM, open circles; 10 μM, closed triangles; 20 μM, open triangles; 50 μM, closed squares; 100 μM, open squares) for various lengths of time. The solid lines represent the best fits to the exponential equation. (B) The k_{obs} values were graphed as a function of dCTP concentration, and the solid line represents the best fit to the hyperbolic equation with k_{pol} equal to 0.0032 $\pm$ 0.0002 s^{-1} and K_d equal to 28 $\pm$ 4 μM. (C) Preincubated Rev1p (100 nM) and DNA containing an 8-oxoG template (100 nM) were mixed with dCTP (10 μM, closed circles; 20 μM, open circles; 50 μM, closed triangles; 100 μM, open triangles; 200 μM, closed squares; 500 μM, open squares) for various lengths of time. The solid lines represent the best fits to the exponential equation. (D) The k_{obs} values were graphed as a function of dCTP concentration, and the solid line represents the best fit to the hyperbolic equation with k_{pol} equal to 0.0039 $\pm$ 0.0002 s^{-1} and K_d equal to 210 $\pm$ 20 μM.

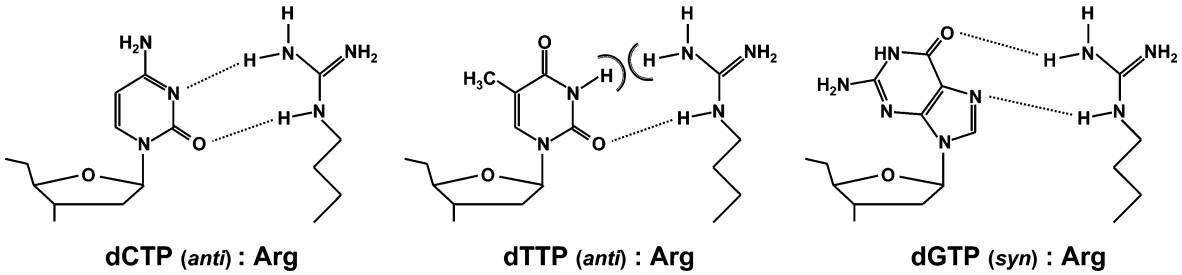

FIGURE 5: Proposed interactions between arginine-324 of Rev1p and various incoming nucleotides. The structure of Arg:dCTP(anti) pair was determined from the X-ray crystal structure of Rev1p in a ternary complex with DNA and dCTP (*33*). The proposed structures of the Arg:dTTP(anti) and the Arg:dGTP(syn) pairs are based on the X-ray structures of the *E. coli* MutM DNA glycosylase in binary complexes with DNA (*40*).

analyses have shown that the incorporation of C opposite G is 500-, 270-, and 130-fold more efficient (k_{cat}/K_m) than that opposite an A, T, and C, respectively (*29*). In this paper, we have also examined how and at which steps along the reaction pathway the template residue influences the efficiency of nucleotide incorporation.

Mechanism of Incoming dNTP Selection. To better understand the mechanism of incoming dNTP selection at the nucleotide-binding step, we measured the K_d for the various incoming dNTPs binding to the Rev1p-DNA binary complex. In these experiments, we used DNA substrates containing a G in the template position, which is the optimal nucleotide in this position. We found that dCTP is bound with 350- and 260-fold greater affinity than dGTP and dTTP, respectively. Thus, although Rev1p utilizes a protein template rather than a DNA template, the impact on dNTP selection at the nucleotide-binding step is similar to that observed with a large number of other DNA polymerases.

In order to better understand the mechanism of nucleotide selection at the nucleotide-incorporation step, we also measured the maximal first-order rate constant of nucleotide incorporation (k_{pol}) once the various dNTPs are bound to Rev1p. Surprisingly, we found that, once bound, dGTP is incorporated at nearly the same rate as is dCTP, and dTTP is incorporated at an ~3-fold slower rate than dCTP. Consequently, with respect to the selection of dCTP as the incoming nucleotide, there is no discrimination at the nucleotide-incorporation step. For the sake of comparison, the bacteriophage T7 DNA polymerase (*36*, *37*) and the Klenow fragment of *Escherichia coli* DNA polymerase I (*38*,

39), both classical DNA polymerases, discriminate against incorrect nucleotide incorporation at the nucleotide-incorporation step by 2000- and 5,000-fold, respectively. Even specialized pol η discriminates against incorrect nucleotide incorporation by 150-fold at this step (*34*). Thus to our knowledge, Rev1p is the first example of a DNA polymerase that discriminates only at the nucleotide-binding step and not at the nucleotide-incorporation step.

In our experiments, we detected no incorporation of A opposite a G in the template position. On the basis of the fact that the discrimination in the case of the other two incorrect dNTPs was achieved solely at the nucleotide-binding step, we believe that dATP is not incorporated because it binds very weakly (K_d > 5 mM) to the Rev1 protein. As we discuss below, an arginine side chain is capable of strong interactions with cytosine, weak interactions with guanine and thymine, and very weak interactions with adenine. From this, we propose that the specificity of Rev1p for dCTP is purely a matter of ground-state interactions between the incoming dNTP and Arg-324.

Impact of the Template Nucleotide. We also examined the impact of various nucleotides at the template position on the mechanism of dCTP incorporation by Rev1p. At the nucleotide-binding step, we see 130-, 95-, and 45-fold weaker dCTP binding opposite A, T, and C residues in the template position, respectively, relative to a G in the template position. Thus, the identity of the residue at the template position of the DNA can significantly affect the binding affinity of the incoming dCTP. When we examined the impact of these nonoptimal template residues on the mechanism of dCTP incorporation, we found the nucleotide-incorporation step was affected in some cases. When A, T, and C were in the template position of the DNA substrate, we observed that the rate constant for the nucleotide-incorporation step (k_{pol}) was 3.3-, 17-, and 25-fold slower, respectively. Thus, the effect of an A in the template position on the nucleotide-incorporation step is minimal, but the presence of T or C at this position significantly reduces the rate of the nucleotide incorporation.

We have also examined the mechanism of dCTP incorporation opposite two types of DNA lesions: an abasic site and an 8-oxoguanine. Previous studies have shown that DNA containing an abasic site in the position of the template residue is a reasonably good substrate for Rev1p (*27*−*29*). Here we show that relative to incorporation with the optimal template G residue, Rev1p binds dCTP opposite an abasic site 46-fold weaker and incorporates the bound nucleotide 2-fold slower. By contrast, prior studies have shown that 8-oxoguanine is not a very good template residue for Rev1p (*29*). We determined that the binding affinity for dCTP opposite 8-oxoguanine is 280-fold weaker than opposite G and that the rate constant for nucleotide incorporation is 3.6-fold slower with 8-oxoguanine than with G as the template residue. Thus, an 8-oxoguanine has a similar effect on the mechanism of nucleotide incorporation as a nonoptimal, undamaged residue in the template position.

Overall, the effects of templating residues other than a G, including abasic and 8-oxoguanine lesions, on dCTP incorporation are much more pronounced at the nucleotide binding step (K_d) than at the nucleotide incorporation step (k_{pol}). These observations are partially explained by the Rev1p ternary structure (*33*): dCTP is efficiently incorporated opposite template G because of the optimal hydrogen bonding of Arg-324 with dCTP and also because template G is well-accommodated in the G loop by hydrogen bonding of the "Hoogsteen edge" of template G with the residues on the G loop of Rev1p. The replacement of template G with any other residue will result in the loss of these hydrogen-bonding interactions as well as in steric problems. For example, an A or an 8-oxoguanine at the templating position will result in the loss of hydrogen-bonding interactions as well as in steric clashes with residues in the G loop. Such interactions between nonoptimal template residue and the G loop must affect the arrangement of amino acid residues at the binding site for the incoming dCTP. An understanding of the precise nature of the structural changes at the nucleotide binding site induced by nonoptimal template residues awaits high-resolution structures of Rev1p bound to DNA substrates with other template residues.

Structural Predictions for Other Rev1 Protein Ternary Complexes. The X-ray crystal structure of the Rev1p ternary complex showed that upon DNA binding, Rev1p flips the template G out of the double helix and interacts with the incoming dCTP (the base that was to pair with this extrahelical G) via an arginine side chain (*33*). This is reminiscent of the protein−DNA interactions observed with the *E. coli* MutM protein, a DNA glycosylase that removes 8-oxoguanine bases from duplex DNA (*40*). To carry out its reaction, MutM flips the 8-oxoguanine out of the DNA double helix into a recognition pocket. The "estranged base", the base that was paired with the 8-oxoguanine, forms hydrogen bonds with the side chain of Arg-112 of MutM (*40*). What is interesting is that interactions between this arginine and the estranged base are critical for efficient catalysis. When the estranged base is a C, removal of the 8-oxoguanine is very efficient. However, when the estranged base is a G or a T, removal of the 8-oxoguanine is slow. There is no detectible removal of the 8-oxoguanine when the estranged base is an A. This latter point is important biologically, because A is incorporated opposite 8-oxoguanine by many DNA polymerases, and the removal of 8-oxoguanine in this sequence context could give rise to G:C to T:A transversion mutations.

X-ray crystal structures exist for the MutM protein bound to DNA substrates containing C, G, and T as the estranged base (*40*). With the optimal substrate (C as the estranged base), the cytosine is in the normal anti configuration and the ϵ and ζ nitrogen atoms of Arg-112 form hydrogen bonds with the O^2 and N3 of the cytosine base, respectively (Figure 5). With the less optimal substrate containing an estranged T, the thymine is also in the normal anti configuration and the ϵ nitrogen of Arg-112 forms a hydrogen bond with the O^2 of the thymine (Figure 5). This interaction, however, is weaker because of a steric clash between the protonated ζ nitrogen of Arg-112 and the protonated N3 atom of the thymine. Interactions with the estranged G are also weaker, because the guanine base is in the less optimal syn conformation. In this case, hydrogen bonds form between the ϵ and ζ nitrogen atoms of Arg-112 and the N7 and O^6 of the guanine, respectively (Figure 5). An estranged A does not interact with Arg-112 presumably because (i) it would have to be in the less optimal syn conformation and (ii) there would be a steric clash between the protonated ζ nitrogen of Arg-112 and the protonated N^6 of the adenine.

On the basis of our pre-steady-state kinetic analyses reported here, we suggest that the interactions observed between Arg-112 and the various estranged bases in MutM could be similar to the interactions in Rev1p between Arg-324 and the various incoming dNTPs (Figure 5). In the case of incoming dCTP, this has already been demonstrated (*33*). We have shown here that dGTP and dTTP bind Rev1p weaker than dCTP binds, and this is consistent with the mode of interactions between Arg-324 and these other dNTPs shown in Figure 5. Moreover, we have argued that dATP binds the Rev1p−DNA binary complex with much lower affinity, and this lends additional support to this proposal.

REFERENCES

1. Echols, H., and Goodman, M. F. (1991) Fidelity mechanisms in DNA replication, *Annu. Rev. Biochem. 60*, 477−511.
2. Goodman, M. F., and Tippin, B. (2000) Sloppier copier DNA polymerases involved in genome repair, *Curr. Opin. Genet. Gev. 10*, 162−168.
3. Prakash, S., and Prakash, L. (2002) Translesion DNA synthesis in eukaryotes: A one- or two-polymerase affair, *Genes Dev. 16*, 1872−1883.
4. Prakash, S., Johnson, R. E., and Prakash, L. (2005) Eukaryotic translesion synthesis DNA polymerases: Specificity of structure and function, *Annu. Rev. Biochem. 74*, 317−353.
5. Washington, M. T., Helquist, S. A., Kool, E. T., Prakash, L., and Prakash, S. (2003) Requirement of Watson−Crick hydrogen bonding for DNA synthesis by yeast DNA polymerase *η*, *Mol. Cell. Biol. 23*, 5107−5112.
6. Wolfle, W. T., Washington, M. T., Kool, E. T., Spratt, T. E., Helquist, S. A., Prakash, L., and Prakash, S. (2005) Evidence for a Watson−Crick hydrogen bonding requirement in DNA synthesis by human DNA polymerase *κ*, *Mol. Cell. Biol. 25*, 7137−7143.
7. Lone, S., Townson, S. A., Uljon, S. N., Johnson, R. E., Brahma, A., Nair, D. T., Prakash, S., Prakash, L., and Aggarwal, A. K. (2007) Human DNA polymerase *κ* encircles DNA: Implications for mismatch extension and lesion bypass, *Mol. Cell 25*, 601−614.
8. Washington, M. T., Johnson, R. E., Prakash, S., and Prakash, L. (1999) Fidelity and processivity of *Saccharomyces cerevisiae* DNA polymerase *η*, *J. Biol. Chem. 274*, 36835−36838.
9. Washington, M. T., Johnson, R. E., Prakash, S., and Prakash, L. (2000) Accuracy of thymine-thymine dimer bypass by *Saccharomyces cerevisiae* DNA polymerase *η*, *Proc. Natl. Acad. Sci. U.S.A. 97*, 3094−3099.
10. Johnson, R. E., Washington, M. T., Prakash, S., and Prakash, L. (2000) Fidelity of human DNA polymerase *η*, *J. Biol. Chem. 275*, 7447−7450.
11. Washington, M. T., Prakash, L., and Prakash, S. (2003) Mechanism of nucleotide incorporation opposite a thymine−thymine dimer by yeast DNA polymerase *η*, *Proc. Natl. Acad. Sci. U.S.A. 100*, 12093−12098.
12. Haracska, L., Yu, S. L., Johnson, R. E., Prakash, L., and Prakash, S. (2000) Efficient and accurate replication in the presence of 7,8-dihydro-8-oxoguanine by DNA polymerase *η*, *Nat. Genet. 25*, 458−461.
13. Carlson, K. D., and Washington, M. T. (2005) Mechanism of efficient and accurate nucleotide incorporation opposite 7,8-dihydro-8-oxoguanine by Saccharomyces cerevisiae DNA polymerase *η*, *Mol. Cell. Biol. 25*, 2169−2176.
14. Trincao, J., Johnson, R. E., Escalante, C. R., Prakash, S., Prakash, L., and Aggarwal, A. K. (2001) Structure of the catalytic core of *S. cerevisiae* DNA polymerase *η*: Implications for translesion DNA synthesis, *Mol. Cell 8*, 417−426.
15. Washington, M. T., Minko, I. G., Johnson, R. E., Wolfle, W. T., Harris, T. M., Lloyd, R. S., Prakash, S., and Prakash, L. (2004) Efficient and error-free replication past a minor-groove DNA adduct by the sequential action of human DNA polymerases *ι* and *κ*, *Mol. Cell. Biol. 24*, 5687−5693.
16. Wolfle, W. T., Johnson, R. E., Minko, I. G., Lloyd, R. S., Prakash, S., and Prakash, L. (2006) Replication past a trans-4-hydroxynonenal minor-groove adduct by the sequential action of human DNA polymerases *ι* and *κ*, *Mol. Cell. Biol. 26*, 381−386.
17. Carlson, K. D., Johnson, R. E., Prakash, L., Prakash, S., and Washington, M. T. (2006) Human DNA polymerase *κ* forms nonproductive complexes with matched primer termini but not with mismatched primer termini, *Proc. Natl. Acad. Sci. U.S.A. 103*, 15776−15781.
18. Uljon, S. N., Johnson, R. E., Edwards, T. A., Prakash, S., Prakash, L., and Aggarwal, A. K. (2004) Crystal structure of the catalytic core of human DNA polymerase *κ*, *Structure 12*, 1395−1404.
19. Johnson, R. E., Washington, M. T., Haracska, L., Prakash, S., and Prakash, L. (2000) Eukaryotic polymerase *ι* and *ζ* act sequentially to bypass DNA lesions, *Nature 406*, 1015−1019.
20. Zhang, Y., Yuan, F., Wu, X., Taylor, J. S., and Wang, Z. (2001) Response of human DNA polymerase *ι* to DNA lesions, *Nucleic Acids Res. 29*, 928−935.
21. Tissier, A., Frank, E. G., McDonald, J. P., Iwai, S., Hanaoka, F., and Woodgate, R. (2000) Misinsertion and bypass of thymine−thymine dimers by human DNA polymerase *ι*, *EMBO J. 19*, 5259−5266.
22. Nair, D. T., Johnson, R. E., Prakash, S., Prakash, L., and Aggarwal, A. K. (2004) Replication by human DNA polymerase *ι* occurs by Hoogsteen base-pairing, *Nature 430*, 377−380.
23. Nair, D. T., Johnson, R. E., Prakash, L., Prakash, S., and Aggarwal, A. K. (2005) Human DNA polymerase *ι* incorporates dCTP opposite template G via a G.C + Hoogsteen base pair, *Structure 13*, 1569−1577.
24. Johnson, R. E., Prakash, L., and Prakash, S. (2005) Biochemical evidence for the requirement of Hoogsteen base pairing for replication by human DNA polymerase *ι*, *Proc. Natl. Acad. Sci. U.S.A. 102*, 10466−10471.
25. Johnson, R. E., Haracska, L., Prakash, L., and Prakash, S. (2006) Role of Hoogsteen edge hydrogen bonding at template pruines in nucleotide incorporation by human DNA polymerase *ι*, *Mol. Cell Biol. 26*, 6435−6441.
26. Nair, D. T., Johnson, R. E., Prakash, L., Prakash, S., and Aggarwal, A. K. (2006) Hoogsteen base pair formation promotes synthesis opposite the 1,N6-ethenodeoxyadenosine lesion by human DNA polymerase *ι*, *Nature Struct. Mol. Biol. 13*, 619−625.
27. Nelson, J. R., Lawrence, C. W., and Hinkle, D. C. (1996) Deoxycytidyl transferase activity of yeast REV1 protein, *Nature 382*, 729−731.
28. Haracska, L., Unk, I., Johnson, R. E., Johansson, E., Burgers, P. M., Prakash, S., and Prakash, L. (2001) Roles of DNA polymerases *δ* and *ζ* and of Rev1 in the bypass of abasic sites, *Genes Dev. 15*, 945−954.
29. Haracska, L., Prakash, S., and Prakash, L. (2002) Yeast Rev1 protein is a G template-specific DNA polymerase, *J. Biol. Chem. 277*, 15546−15551.
30. Zhang, Y., Wu, X., Rechkoblit, O., Geacintiv, N. E., Taylor, J. S., and Wang, Z. (2002) Response of human REV1 to different DNA damage: Preferential dCMP insertion opposite the lesion, *Nucleic Acids Res. 30*, 1630−1638.
31. Masuda, Y., and Kamiya, K. (2002) Biochemical properties of human REV1 protein, *FEBS Lett. 520*, 88−92.
32. Washington, M. T., Minko, I. G., Johnson, R. E., Haracska, L., Harris, T. M., Lloyd, R. S., Prakash, S., and Prakash, L. (2004) Efficient and error-free replication past a minor-groove N^2-guanine adduct by the sequential action of yeast Rev1 and DNA polymerase *ζ*, *Mol. Cell. Biol. 24*, 6900−6906.
33. Nair, D. T., Johnson, R. E., Prakash, L., Prakash, S., and Aggarwal, A. K. (2005) Rev1 employs a novel mechanism of DNA synthesis using a protein template, *Science 309*, 2219−2222.
34. Washington, M. T., Prakash, L., and Prakash, S. (2001) Yeast DNA polymerase *η* utilizes an induced-fit mechanism of nucleotide incorporation, *Cell 107*, 917−927.
35. Washington, M. T., Johnson, R. E., Prakash, L., and Prakash, S. (2004) Human DNA polymerase *ι* utilizes different nucleotide incorporation mechanisms dependent upon the template base, *Mol. Cell. Biol. 24*, 936−943.
36. Patel, S. S., Wong, I., and Johnson, K. A. (1991) Pre-steady-state kinetic analysis of processive DNA replication including complete characterization of an exonuclease-deficient mutant, *Biochemistry 30*, 511−525.
37. Wong, I., Patel, S. S., and Johnson, K. A. (1991) An induced-fit kinetic mechanism for DNA replication fidelity: Direct measurement by single-turnover kinetics, *Biochemistry 30*, 526−537.

38. Kuchta, R. D., Mizrahi, V., Benkovic, P. A., Johnson, K. A., and Benkovic, S. J. (1987) Kinetic mechanism of DNA polymerase I (Klenow), *Biochemistry 26*, 8410−8417.
39. Kuchta, R. D., Benkovic, P., and Benkovic, S. J. (1988) Kinetic mechanism whereby DNA polymerase I (Klenow) replicates DNA with high fidelity, *Biochemistry 27*, 6716−6725.
40. Fromme, J. C., and Verdine, G. L. (2002) Structural insights into lesion recognition and repair by the bacterial 8-oxoguanine DNA glycosylase MutM, *Nat. Struct. Biol. 9*, 544−552.

BI701429V